J Mol Model (2014) 20:2475
DOI 10.1007/s00894-014-2475-2

ORIGINAL PAPER

Theoretical investigation on mechanism and kinetics of the Cl-initiated hydrogen abstraction reactions of ethyl trifluoroacetate at 298 K

Bhupesh Kumar Mishra · Hari Ji Singh · Laxmi Tiwari

Received: 7 April 2014 / Accepted: 21 September 2014 / Published online: 11 October 2014

Abstract Theoretical investigations were carried out on the gas-phase reactions of $CF_3C(O)OCH_2CH_3$, ethyl trifluoroacetate (ETFA) with Cl atoms by means of modern density functional theory methods. The optimized geometries, frequencies and minimum energy path were obtained with the hybrid density functional model MPWB1K using the 6-31+G(d,p) basis set. The single point energy calculations were refined further using the G2(MP2) method. Two conformers relatively close in energy were identified for ETFA; both are likely to be important in the temperature range of our study. The existence of transition states on the corresponding potential energy surface was ascertained by performing intrinsic reaction coordinate calculations. The rate constant at 298 K calculated theoretically using canonical transition state theory was found to be in good agreement with experimentally measured values. Our calculations suggest that H abstraction from the $–CH_2$ group is kinetically and thermodynamically more favorable than abstraction from the $–CH_3$ group. The atmospheric lifetime of ETFA with Cl atoms was determined to be 1.98 years. To the best of our knowledge, this work represents the first determination of the rate coefficients for the gas-phase reaction of chlorine atoms in ETFA.

Keywords Fluoroester · Hydrogen abstraction · Conformer · Canonical transition state theory · Atmospheric lifetime

B. K. Mishra (✉)
Department of Chemical Sciences, Tezpur University, Tezpur, Napaam, Assam 784 028, India
e-mail: bhupesh@tezu.ernet.in

B. K. Mishra
e-mail: bhupesh_chem@rediffmail.com

H. J. Singh · L. Tiwari
Department of Chemistry, D.D.U. Gorakhpur University, Gorakhpur, Uttar Pradesh 273009, India

Introduction

Recently, volatile organic compounds (VOCs), especially hydrofluoroethers (HFEs), have been designed and are widely recommended as a third generation replacement for chlorofluorocarbons (CFCs), Hydrofluorocarbon (HFCs) and hydrochlorofluorocarbon (HCFCs) can be used in applications such as cleaning of electronic equipment, heat transfer fluid in refrigerators, lubricant deposition and foam blowing agents [1–3]. The major degradation pathways of HFEs in the atmosphere may be initiated by photolytic degradation with OH radicals and Cl atoms in coastal areas and also possibly with chloride-containing aerosols in highly industrialized urban areas. It is well established that the OH- and Cl-initiated oxidation of HFEs generate the homologous fluorinated esters (FESs) as the primary products [4–6]. For instance, the fluoroakylformates $C_4F_9OC(O)H$ and n-$C_3F_7OC(O)H$ are the major degradation products of HFE-7100 ($C_4F_9OCH_3$) and HFE-7000 ($C_3F_7OCH_3$), respectively [5, 7]. Like most VOCs, reaction with OH radicals is considered to be the dominant process removing esters from the troposphere [8]. Although global atmospheric abundance of OH radicals is around two orders of magnitude greater than that of chlorine atoms, Cl reactions are generally faster than OH reactions, so their contribution to the degradation of VOCs may be not negligible compared to the role of OH radicals [9]. This contribution of Cl could be significant in areas where the concentration of Cl precursor species has been reported to be high, such as the coastal boundary layer [10]. In fact, chlorine atoms have been monitored in concentrations on the order of 10^4 molecule cm^{-3} over the marine boundary layer [11]. Thus, chlorine atoms also play an important role in atmospheric chemistry [12]. It has been reported recently that fluorinated esters can be used as potential solvents or co-solvents for Li-ion batteries [13–15]. Among fluorinated esters, methyl difluoroacetate based electrolyte showed the best electrochemical

properties and the highest thermal stability coexisting with Li metal [16]. Recently, Lu et al. [17] reported that ethyl trifluoroacetate is suitable as a co-solvent of rechargeable lithium-ion battery electrolyte for low temperature use. A high cycling efficiency of lithium metal has been reported using CF_3SO_3Li/ethyltrifluoroacetate+methyl acetate [18]. The degradation of FESs leads to the formation of trifluoroacetic acid (TFA) acid and the corresponding anhydride along with CF_2O and CO_2 and HF as hydrolysis products. It has been also reported that TFA detected in surface waters has no known sink apart from rainwater, and that this species may impact on agricultural and aquatic systems [19]. Therefore, it is necessary to understand the chemistry of fluorinated esters in the atmosphere in order to assess the environmental acceptability of HFEs as a plausible replacement for chlorofluorocarbons. The reaction mechanisms of FESs with atmospheric oxidants have been studied extensively both experimentally [20–25] and theoretically [26–32] and continue to receive considerable attention. FESs absorb strongly in the earthly infrared (IR) radiation region of 800–1,200 cm^{-1}. Recently, theoretical IR spectra for a set of perfluorocarbons were determined by Bravo et al. [4] using density functional theory (DFT) methods. The indirect global warming potential (GWP) was calculated using the radiative efficiencies and lifetimes of the HFE and its degradation FES products. Lestard et al. [33] determined the molecular structure of two conformers of ETFA in the gas-phase by electron-diffraction supplemented by ab initio (MP2) and DFT calculations using 6-311++G(d,p) basis set. The present study will focus on reaction rate constants as well as the mechanistic aspects of $CF_3C(O)OCH_2CH_3$+Cl reactions. With respect to reactant $CF_3C(O)OCH_2CH_3$, two stable conformers (SC1 and SC2) were identified. The SC1 conformer was found to be more stable than the SC2 conformer by about 0.17 kcal mol^{-1} with the G2(MP2) method and 0.37 kcal mol^{-1} at the MPWB1K/6-31+G(d,p) level. The small energy difference between these implies that both may contribute to the title reaction by weight factors estimated from the Boltzmann distribution function. Our calculation indicates that two reaction channels each from $–CH_3$ and $–CH_2$ group are feasible for both the SC1 and SC2 conformers as given below:

$$CF_3C(O)OCH_2CH_3 + Cl \rightarrow CF_3C(O)OCH_2CH_2 + HCl \quad (1)$$

$$CF_3C(O)OCH_2CH_3 + Cl \rightarrow CF_3C(O)OCHCH_3 + HCl \quad (2)$$

Blanco et al. [21] studied the kinetics of hydrogen abstraction reactions with Cl atoms for ETFA at (298±2) K and atmospheric pressure (760±10 Torr) using in situ Fourier transform (FT)-IR spectroscopy. The experimental rate constants was derived as $k(Cl+CF_3C(O)OCH_2CH_3)=(1.78\pm0.57)\times10^{-12}$ cm^3 $molecule^{-1}$ s^{-1}. To the best of our knowledge, no theoretical study to date has focused on the title reaction to understand its mechanism and thermochemistry. Therefore, as a supplement to experiments, we here present an extensive theoretical study on the reaction of ETFA with Cl atoms to reveal mechanistic details that are not accessible directly from experimental research. The present study may help us understand the title reaction more comprehensively.

Computational methods

Geometry optimization of the reactants, products and transition states were made at the MPWB1K level of theory [34] using the 6-31+G(d,p) basis set. The MPWB1K/6-31+G(d,p) method was reported in earlier studies [35–38] to be sufficiently accurate for predicting reliable geometries and frequencies of the stationary points. The 6-31+G(d,p) basis set was used because the same basis set was used for developing the model functional. The unrestricted formalism was used for quantum chemical calculations of the open-shell TS and radicals. The $<S^2>$ value never exceeded 0.761, indicating that spin-contamination was not serious for the present system. In order to determine the nature of different stationary points on the potential energy surface, vibrational frequencies calculations were performed using the same level of theory at which the optimization was made. All the stationary points were identified to correspond to stable minima by ascertaining that all the vibrational frequencies had real positive values. The transition states were characterized by the presence of only one imaginary frequency (NIMAG=1). To ascertain that the identified transition states connect reactant and products smoothly, intrinsic reaction coordinate (IRC) calculations [39] were performed at the MPWB1K/6-31+G(d,p) level. As the reaction energy barriers are very sensitive to theoretical level, the higher-order correlation corrected relative energies along with the density functional energies were necessary to obtain theoretically consistent reaction energies. Therefore, a potentially high-level method such as G2(MP2) was used for single-point energy calculations.

The G2(MP2) [40] energy was calculated in the following manner:

$$E[G2(MP2)] = E_{base} + \Delta E(MP2) + HLC + ZPE$$

where E_{base}=E[QCISD(T)/6-311G(d,p)], ΔE(MP2)=E[MP2/6-311+G(3df,2p)]−E[MP2/6-311G(d,p)], and HLC (high level correction)=$-0.00481n_\beta-0.00019n_\alpha$ (n_α and n_β are the number of α and β valence electrons with $n_\alpha \geq n_\beta$) and ZPE = zero-point energy.

In this method, the geometry and frequency calculations were performed at MPWB1K/6-31+G(d,p) level. The ZPE thus obtained was corrected with a scale factor of 0.951 to partly eliminate systematic errors [34]. This dual level calculation [G2(MP2)//MPWB1K/6-31+G(d,p)] is known to produce reliable thermochemical and kinetic data [28, 41–44]. All quantum mechanical calculations were performed with the Gaussian 09 suite of programs [45]. As mentioned, the two most stable conformers (SC1 and SC2) of $CF_3C(O)OCH_2CH_3$ are very close in energy. Therefore, any thermodynamic quantity (Q) for $CF_3C(O)OCH_2CH_3$ at temperature T was estimated from the weighted average of that quantity for the SC1 (Q_{SC1}) and SC2 (Q_{SC2}) conformers of $CF_3C(O)OCH_2CH_3$ as:

$$Q = W_{SC1}.Q_{SC1} + W_{SC2}.Q_{SC2} \quad (3)$$

where W_{SC1} and W_{SC2} are the temperature dependent weight factors according to the Boltzmann distribution law [46].

Results and discussion

Geometry optimization of the ETFA molecule predicts two possible conformers (SC1 and SC2) and their structures are shown in Fig. 1. The two conformers differ mainly in the orientation of C3–H1 bond relative to the C–O–C–C backbone. The C2–O1–C3–C4 dihedral angle is 177.71 in the SC1 conformer; whereas this angle is 81.27 in the SC2 conformer. Quantum mechanical analysis on the energies of these two conformers shows that SC1 conformer is the most stable conformation of the ETFA molecule, which is in accord with the observation reported by Lestard et al. [33]. Since these two conformers are close in energy (0.17 kcal mol^{-1}), both (SC1 and SC2) need to be considered while studying reactions 1–2.

The calculated enthalpy of reactions ($\Delta_rH°_{298}$) and reaction free energies ($\Delta_rG°_{298}$) at 298 K for the reactions of ETFA with Cl atoms are listed in Table 1. Free energy values show that both reactions are exergonic ($\Delta_rG°_{298}<0$) and thus thermodynamically facile. The $\Delta_rH°_{298}$ values given in Table 1 for reactions (1–2) show that hydrogen abstraction from the $–CH_2$ group is more exothermic than that from the $–CH_3$ group. There are two potential hydrogen abstraction sites of $CF_3C(O)OCH_2CH_3$, namely the $–CH_3$ and $–CH_2$ groups. However, as can be seen from the geometrical parameters and stereographical orientation, the hydrogen atoms in the $–CH_3$ and $–CH_2$ groups are equivalent. Two transition states (TSs) are therefore located for reactions of SC1 with Cl atoms; one TS ($TS1_{SC1}$) for H-abstraction from the $–CH_3$ group and one TS for the same from the $–CH_2$ group ($TS2_{SC2}$). Similarly, two transition states ($TS1_{SC2}$ and $TS2_{SC2}$) are located for reactions of SC2 conformers of ETFA. Therefore, a total of four transition states are located for reaction channels (1–2).

The optimized geometries for species involved in reaction channels (1–2) are shown in Fig. 1. Transition state searches were made along the minimum energy path on a relaxed potential energy surface. In the process of the hydrogen abstraction reaction from a C–H bond, the C–H bond breaks and a new O–H bond is formed, giving rise to the water molecule. Thus, during the formation of transition states, the important structural parameters that have to be observed are one of the C–H bonds of the leaving hydrogen and the newly formed bond between H and O atoms in the OH radical. Visualization of the optimized structures of transition states ($TS1_{SC1}$, $TS2_{SC1}$, $TS1_{SC2}$ and $TS2_{SC2}$) further reveals that elongation of the breaking C–H bond length is longer in the range of 23.66 % to 35.39 % whereas the newly formed H–Cl bond is longer by 10.53 % to 16.90 % than the H–Cl bond length in the isolated HCl molecule. This indicates that the barrier of reactions (1–2) lies near the product, and the reaction with Cl atoms will proceed via a late transition state.

Results obtained during frequency calculations for species involved in reactions (1–2) are recorded in Table 2. These results show that the reactants and products have stable minima on their potential energy surface characterized by the occurrence of only real positive vibrational frequencies. Transition states (TSs) are characterized by the occurrence of only one imaginary frequency at 705i, 886i, 736i and 898 cm^{-1} for $TS1_{SC1}$, $TS2_{SC1}$, $TS1_{SC2}$ and $TS2_{SC2}$, respectively, at MPWB1K level of theory. Visualization of the vibration corresponding to the calculated imaginary frequencies shows a well defined TS geometry connecting reactants and products during transition. The existence of a TS on the potential energy surface was further ascertained by IRC calculations performed at the same level of theory that clearly authenticate a smooth transition from reactants to products on the potential energy surface. Single-point energy calculations of various species involved in the hydrogen abstraction reactions were performed with the G2(MP2) method using MPWB1K/6-31+G(d,p) optimized geometries.

The associated energy barrier corresponding to reactions (1–2) calculated from the results obtained at the two above-mentioned theoretical levels are recorded in Table 3. These results show that energy barriers for H atom abstraction by Cl atoms from the SC1 conformer from the $–CH_3$ group were 2.60 and 4.13 kcal mol^{-1} at G2(MP2) and MPWB1K/6-31G+(d,p) levels of theory, respectively. On the other hand, the same from the $–CH_2$ group were found to be 1.67 and 2.81 kcal mol^{-1} at G2(MP2) and MPWB1K/6-31G+(d,p) levels of theory, respectively. Similarly, the energy barriers for SC2 conformer from the $–CH_3$ and $–CH_2$ groups were found to be 3.06 and 1.89 kcal mol^{-1}, respectively with the G2(MP2) method. The MPWB1K/6-31G+(d,p) results were 3.84 and 2.01 kcal mol^{-1}, respectively, for $–CH_3$ and $–CH_2$ groups of the SC2 conformer. A literature survey revealed that there is no experimental data available for comparison of the

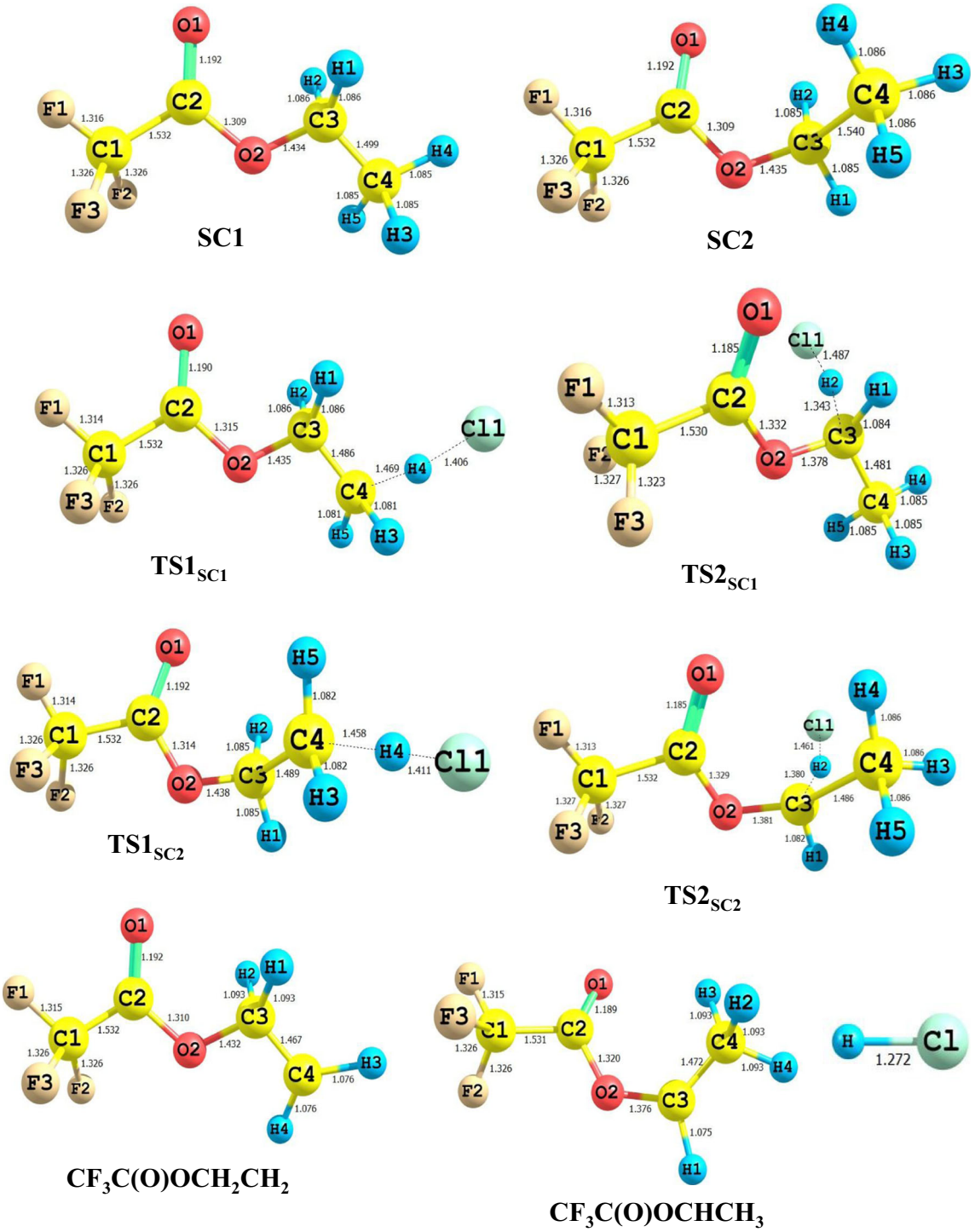

Fig. 1 Optimized geometries of reactants, products and transitions states at MPWB1K level of theory. Bond lengths are in Ångstroms

energy barrier for the H-atom abstraction reaction of ETFA by Cl atoms. A potential energy diagram of the title reactions was constructed with the results obtained at G2(MP2)//MPWB1K/6-31G+(d,p) level of theory and is shown in Fig. 2. These energies are plotted with respect to the ground state energy of reactants ($CF_3C(O)OCH_2CH_3$+Cl) arbitrarily taken as zero. The values in parentheses in Fig. 2 are ZPE corrected values obtained at MPWB1K/6-31+G(d,p) level. The barrier height values show that hydrogen abstraction by Cl atoms from the –CH_2 group is easier than that from the –CH_3 group. This finding is in accord with the mechanism proposed by Blanco et al. [22], which is based on his experimental observation that reaction of $CF_3C(O)OCH_2CH_3$+Cl proceeds mainly from the –CH_2 site.

Table 1 Thermochemical data at G2(MP2) and MPWB1K levels of theory. All values are in kcal mol^{-1}

Conformer	Reaction channel	$\Delta_rH°_{298}$		$\Delta_rG°_{298}$	
		G2(MP2)	MPWB1K	G2(MP2)	MPWB1K
SC1	1	0.06	2.32	−2.76	−0.49
	2	−1.70	−3.39	−4.00	−5.67
SC2	1	−0.02	2.05	−2.85	−1.33
	2	−1.77	−3.65	−4.63	−6.51
	Average 1[a]	0.02	2.20	−2.79	−0.85
	Average 2[a]	−1.73	−3.50	−4.27	−6.03

[a] Weighted average as per Boltzmann distribution law as given in Eq. (3)

Table 2 Harmonic vibrational frequencies of reactants, products and transition states at MPWB1K/6-31+G(d,p) level of theory

Species	Vibrational frequencies (cm^{-1})
SC1	18, 51, 116, 128, 247, 279, 298, 346, 397, 448, 534, 600, 760, 808, 828, 908, 932, 1,097, 1,169, 1,204, 1,253, 1,267, 1,328, 1,329, 1,413, 1,456, 1,496, 1,516, 1,529, 1,550, 1,946, 3,135, 3,154, 3,205, 3,224, 3,234
SC2	22, 75, 103, 1,751, 12,412, 2,158, 338, 362, 4,219, 468, 537, 598, 754, 83, 818, 900, 921, 1,085, 1,151, 1,211, 1,252, 1,268, 1,328, 1,364, 1,417, 1,454, 1,490, 1,519, 1,530, 1,541, 1,944, 3,133, 3,173, 3,221, 3,224, 3,248
$TS1_{SC1}$	705i, 19, 24, 46, 50, 115, 132, 281, 283, 322, 393, 396, 446, 533, 601, 618, 761, 803, 809, 821, 891, 918, 1,028, 1,131, 1,198, 1,225, 1,240, 1,271, 1,321, 1,332, 1,412, 1,475, 1,512, 1,540, 1,952, 3,163, 3,209, 3,224, 3,319
$TS2_{SC1}$	886i, 25, 35, 49, 126, 129, 159, 216, 281, 284, 358, 395, 439, 495, 532, 604, 761, 798, 822, 901, 957, 1,048, 1,060, 1,178, 1,194, 1,231, 1,247, 1,276, 1,339, 1,402, 1,442, 1,468, 1,503, 1,508, 1,968, 3,118, 3,208, 3,223, 3,247
$TS1_{SC2}$	736i, 26, 28,42, 83, 104, 188, 241, 325, 356, 415, 428, 459, 536, 598, 614, 756, 801, 815, 816, 894, 909, 1,017, 1,111, 1,204, 1,216, 1,250, 1,272, 1,332, 1,360, 1,417, 1,476, 1,502, 1,538, 1,948, 3,183, 3,210, 3,256, 3,322
$TS2_{SC2}$	898i, 29, 39, 66, 110, 143, 163, 222, 259, 300, 356, 425, 444, 513, 538, 598, 763, 803, 819, 887, 939, 1,021, 1,048, 1,152, 1,171, 1,219, 1,263, 1,275, 1,340, 1,402, 1,445, 1,463, 1,503, 1,521, 1,970, 3,111, 3,212, 3,248, 3,265
$CF_3C(O)OCH_2CH_2$	20, 48, 112, 131, 144, 282, 284, 353, 400, 441, 474, 534, 601, 761, 812, 864, 930, 979, 1,121, 1,166, 1,252, 1,268, 1,275, 1,330, 1,409, 1,478, 1,496, 1,520, 1,946, 3,080, 3,156, 3,258, 3,378
$CF_3C(O)OCHCH_3$	25, 88, 107, 131, 172, 277, 290, 358, 391, 414, 463, 533, 602, 761, 795, 901, 958, 1,021, 1,180, 1,190, 1,254, 1,266, 1,333, 1,401, 1,448, 1,475, 1,495, 1,511, 1,940, 3,075, 3,163, 3,227, 3,329,
HCl	3,084

Rate constants

The rate constant for title reactions were calculated by using canonical transition state theory (CTST) [47] given by the following expression:

$$k = \sigma\Gamma(T)\frac{k_B T}{h}\frac{Q^{\ddagger}_{TS}}{Q_R}\exp\frac{-\Delta E}{RT} \quad (4)$$

Where, σ is the symmetry number, Γ(T) is the tunneling correction factor at temperature T. $Q^{\ddagger}_{TS}$ and Q_R are the total partition function (per unit volume) for the transition states and reactants, respectively. ΔE is the barrier height, k_B is the Boltzmann constant and h is Plank's constant. R represents the universal gas constant. The electronic partition function for Cl atom was evaluated by taking the splitting of 881 cm^{-1} between the ground $^2P_{3/2}$ and excited $^2P_{1/2}$ electronic states of the Cl atom due to spin-orbit coupling. The partition functions for the respective TS and reactants at 298 K are obtained from the vibrational frequencies calculation made at MPWB1K/6-31+G(d,p)

Table 3 Relative energies ΔE (kcal mol^{-1}) with zero-point energy (ZPE) correction for the reactants, transition states (TSs) and products at G2(MP2) and MPWB1K/ 6-31+G(d,p) levels of theory

Species	G2(MP2)	MPWB1K/6-31+G(d,p)
SC1+Cl	0.00	0.00
SC2+Cl	0.17	0.37
$TS1_{SC1}$	2.60	4.13
$TS2_{SC1}$	1.67	2.81
$TS1_{SC2}$	3.06	3.84
$TS2_{SC2}$	1.89	2.01
$CF_3C(O)OCH_2CH_2$+HCl	−0.51	1.74
$CF_3C(O)OCHCH_3$+HCl	−2.21	−3.90

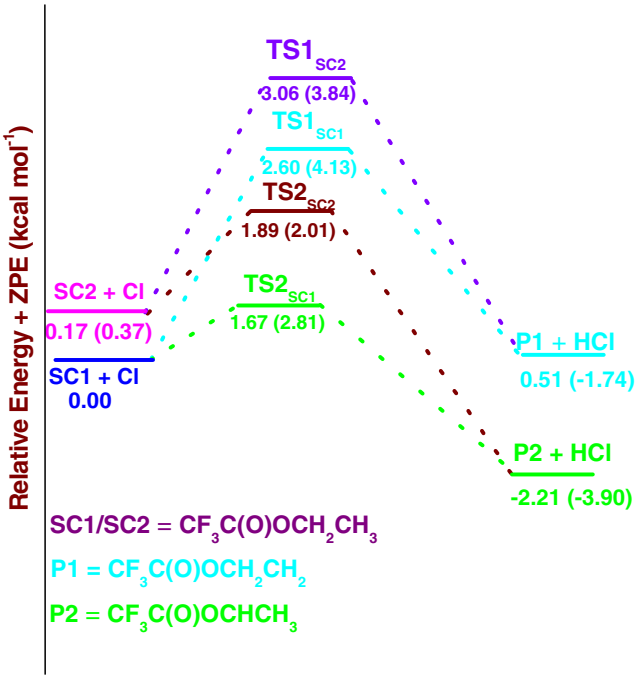

Fig. 2 Schematic potential energy profile for hydrogen abstraction reactions of $CF_3C(O)OCH_2CH_3$ with Cl atoms. Relative energies (in kcal mol^{-1}) of different species are calculated at G2(MP2) and MPWB1K (*in parentheses*) levels of theory

level. The tunneling correction Γ(T) was estimated by using the Eckart's unsymmetric barrier method [48, 49]. In this method, the reaction path through TS is fitted first in a model potential function

$$V = -\frac{Ay}{1-y} - \frac{By}{(1-y)^2} \tag{5}$$

where y=−exp (2πx/L) and A and B are two parameters that depend upon forward and reverse barrier heights. All vibrational modes, except for the lowest vibrational mode, were treated quantum mechanically as separable harmonic oscillators, whereas for the lowest-frequency mode, the partition function was evaluated by the hindered-rotor approximation by Chuang and Truhlar [50] method. Using Truhlar's procedure [51], however, in our case q^{HIN}/q^{HO} ratio was found to be close to one (0.97–0.99). The branching ratios for the H-abstraction reaction channels, which represent the individual contribution of a reaction channel towards overall reaction rate was determined by using the following expression,

$$\text{Branching ratio} = \frac{k_{1/2}}{k_{total}} \times 100 \tag{6}$$

The partial rate coefficients cannot be determined experimentally and the experimental data mostly represent the overall rate constant. That is why theoretical methods can be so valuable for the full understanding of the chemical systems.

As stated earlier, ETFA+Cl reactions pass through two reaction channels (1–2), the contribution from each of these channels needs to be taken into account while calculating the total rate coefficient (k_{Cl}) for the titled reaction. The total rate constant (k_{OH}) at temperature T is then estimated from the weighted average of the rate constant values for k_{SC1} and k_{SC2} as:

$$k(T) = W_{SC1}(T).k_{SC1}(T) + W_{SC2}.k_{SC2}(T) \tag{7}$$

The W_{SC1} and W_{SC2} are the temperature dependent weight factors estimated from the Boltzmann population distribution law [46]. The W_{SC1} is calculated as [1/(1+exp(−ΔE/RT)], where ΔE is the energy difference between the SC1 and SC2 conformer, and $W_{SC2}=1-W_{SC1}$. At 298 K, our calculated k_{Cl} value using G2(MP2) barrier heights is 1.60×10^{-12} cm^3 $molecule^{-1}$ s^{-1} which is in good agreement with the experimental value of $(1.78\pm0.57)\times10^{-12}$ cm^3 $molecule^{-1}$ s^{-1} reported by Blanco et al. [21]. The calculated k_{Cl} value obtained from MPWB1K results is 2.15×10^{-12} cm^3 $molecule^{-1}$ s^{-1}, which is also in reasonably good agreement with the G2(MP2) and experimental values at 298 K. The calculated branching ratio values show that the $–CH_2$ site has greater contribution (90 %) to the overall rate constant, which indicates clearly the dominance of H-abstraction from the $–CH_2$ group of ETFA. Hence our calculation predicts reaction channel (2) as the major reaction channel, which is in accordance with the experimental observation made by Blanco et al. [22].

Atmospheric lifetime

In general, the tropospheric lifetime (τ_{eff}) of ETFA can be estimated by assuming that its removal from troposphere occurs only through the reactions with Cl atoms. Then, (τ_{eff}) can be expressed as [52],

$$\tau_{eff} = \tau_{Cl} \tag{8}$$

where, $\tau_{Cl} = (k_{Cl} \times [Cl])^{-1}$. Using the 298 K value of $k_{Cl}=1.60\times10^{-12}$ cm^3 $molecule^{-1}$ s^{-1} and the global average atmospheric Cl concentrations of 1.0×10^4 molecule cm^{-3} [11], the estimated atmospheric lifetime of ETFA is found to be 1.98 years, which is in good agreement with the value of 2.0 years reported by Blanco et al. [21].

Conclusions

The potential energy surface and reaction kinetics of the Cl-initiated hydrogen abstraction reactions of $CF_3C(O)OCH_2CH_3$ were investigated at G2(MP2)//MPWB1K/6-31+G(d,p) level of theory. Two most stable conformers of the $CF_3C(O)OCH_2CH_3$ molecule (SC1 and SC2) were identified

and their energy difference found to be only 0.17 kcal mol^{-1} with the G2(MP2) method. For each conformer, the possible H-abstraction channels from $–CH_3$ and $–CH_2$ groups were taken into account. The barrier height for dominant pathways is found to be 1.67 kcal mol^{-1} with the G2(MP2) method. The thermal rate constant for the H atom abstraction of $CF_3C(O)OCH_2CH_3$ by Cl atoms was found to be 1.60×10^{-12} cm^3 $molecule^{-1}$ s^{-1} at 298 K using CTST, which is in good agreement with experimental data. From our theoretical study, along with experimental evidence, it can be concluded that hydrogen abstraction from the $–CH_2$ site is both kinetically and thermodynamically more favorable than that from the $–CH_3$ site. The estimated atmospheric life time of ETFA was found to be 1.98 years.

Acknowledgments B.K.M. is thankful to University Grants Commission, New Delhi for awarding a Dr. D. S. Kothari Fellowship. The financial assistance provided by the Council of Scientific and Industrial Research (CSIR), New Delhi is also acknowledged.

References

1. Tsai WT (2005) J Hazard Mater 119:69–78
2. Sekiya A, Misaki S (2000) J Fluorine Chem 101:215–221
3. Powell RL (2002) J Fluor Chem 114:237–250
4. Bravo I, Dıaz-de-Mera Y, Aranda A, Moreno E, Nutt DR, Marston G (2011) Phys Chem Chem Phys 13:17185–17193
5. Ninomiya Y, Kawasaki M, Guschin A, Molina LT, Molina MJ, Wallington TJ (2000) Environ Sci Technol 34(14):2973–2978
6. Nohara K, Toma M, Kutsuna S, Takeuchi K, Ibusuki T (2001) Environ Sci Technol 35(1):114–120
7. Wallington TJ, Schneider WF, Sehested J, Bilde M, Platz J, Nielsen OJ, Christensen LK, Molina MJ, Molina LT, Wooldridge PW (1997) J Phys Chem A 101:8264–8274
8. Chen L, Kutsuna S, Tokuhashi K, Sekiya A (2004) Int J Chem Kinet 36(6):337–344
9. Mera YD, Aranda A, Bravo I, Moreno E, Martinez E, Rodriguez A (2009) Chem Phys Lett 479:20–24
10. Tiu GC, Fu-Ming T (2006) Chem Phys Lett 428:42–48
11. Wingenter OW, Kubo MK, Blake NJ, Smith TW, Blake DR, Rowland FS (1996) J Geophys Res 101:4331–4340
12. Zierkiewicz W (2013) Chem Phys Lett 555:72–78
13. Lu W, Xie K, Chen Z, Pan Y, Zheng C (2014) J Fluor Chem 161:110–119
14. Nakajima T, Dan K, Koh M (1998) J Fluor Chem 87:221–227
15. Chandrasekaran R, Koh M, Ozhawa Y, Aoyoma H, Nakajima T (2009) J Chem Sci 121:339–346
16. Zhao L, Okada S, Yamaki J (2013) J Power Sources 244:369–374
17. Lu W, Xie K, Pan Y, Chen Z, Zheng C (2013) J Fluor Chem 156:136–143
18. Yamakia JI, Yamasaki I, Egashira M, Okada S (2001) J Power Sources 102:288–293
19. Jordan A, Frank H (1999) Environ Sci Technol 33(4):522–527
20. Blanco MB, Teruel MA (2007) Atmos Environ 41(34):7330–7338
21. Blanco MB, Bejan I, Barnes I, Wiesen P, Teruel MA (2008) Chem Phys Lett 453:18–23
22. Blanco MB, Bejan I, Barnes I, Wiesen P, Teruel MA (2010) Environ Sci Technol 44:2354–2359
23. Stein TNN, Christensen LK, Platz J, Sehested J, Nielsen OJ, Wallington TJ (1999) J Phys Chem A 103:5705–5713
24. Blanco MB, Barnes I, Teruel MA (2010) J Phys Org Chem 23:950–954
25. Blanco MB, Rivela C, Teruel MA (2013) Chem Phys Lett 578:33–37
26. Mishra BK, Chakrabatty AK, Deka RC (2014) Struct Chem 25:463–470
27. Chakrabatty AK, Mishra BK, Bhattacharjee D, Deka RC (2013) Mol Phys 111:860–867
28. Mishra BK, Chakrabatty AK, Deka RC (2013) J Mol Model 19:2189–2195
29. Singh HJ, Tiwari L, Rao PK (2014) Bull Korean Chem Soc 35:1385–1390
30. Gour NK, Deka RC, Singh HJ, Mishra BK (2014) J Fluor Chem 160:64–71
31. Mishra BK (2014) RSC Adv 4:16759–16764
32. Zhu P, Ai L-l, Wang H, Liu J-y (2014) Comp Theor Chem 1029:91–98
33. Lestard MED, Tuttolomondo ME, Wann DA, Robertson HE, Rankin DWH, Altabef AB (2010) J Raman Spectrosc 41:1357–1368
34. Zhao Y, Truhlar DG (2004) J Phys Chem A 108:6908–6918
35. Zeegers-Huyskens T, Lily M, Sutradhar D, Chandra AK (2013) J Phys Chem A 117:8010–8016
36. Chakrabartty AK, Mishra BK, Bhattacharjee D, Deka RC (2013) J Fluor Chem 154:60–66
37. Devi KJ, Chandra AK (2011) Chem Phys Lett 502:23–28
38. Mishra BK, Lily M, Chakrabartty AK, Deka RC, Chandra AK (2014) J Fluor Chem 159:57–64
39. Gonzalez C, Schlegel HB (1989) J Chem Phys 90:2154–2161
40. Curtiss LA, Raghavachari K, Pople JA (1993) J Chem Phys 98:1293–1298
41. Mishra BK, Lily M, Deka RC, Chandra AK (2014) J Mol Graph Model 50:90–99
42. Deka RC, Mishra BK (2014) Chem Phys Lett 595–596:43–47
43. Lily M, Sutradhar D, Chandra AK (2013) Comp Theor Chem 1022:50–58
44. Chandra AK (2012) J Mol Model 18:4239–4247
45. Frisch MJ, Trucks GW, Schlegel HB, Scuseria GE, Robb, Cheeseman JR, Scalmani G, Barone V, Mennucci B, Petersson GA, Nakatsuji H, Caricato M, Li X, Hratchian HP, Izmaylov AF, Bloino J, Zheng G, Sonnenberg JL, Hada M, Ehara M, Toyota K, Fukuda R, Hasegawa J, Ishida M, Nakajima T, Honda Y, Kitao O, Nakai H, Vreven T, Montgomery JA Jr, Peralta JE, Ogliaro F, Bearpark M, Heyd JJ, Brothers E, Kudin KN, Staroverov VN, Kobayashi R, Normand J, Raghavachari K, Rendell K, Burant JC, Iyengar SS, Tomasi J, Cossi M, Rega N, Millam JM, Klene M, Knox JE, Cross JB, Bakken V, Adamo C, Jaramillo J, Gomperts R, Stratmann RE, Yazyev O, Austin AJ, Cammi R, Pomelli C, Ochterski JW, Martin RL, Morokuma K, Zakrzewski VG, Voth GA, Salvador P, Dannenberg JJ, Dapprich S, Daniels AD, Farkas O, Foresman JB, Ortiz JV, Cioslowski J, Fox DJ (2010) Gaussian 09, revision B.01. Gaussian Inc, Wallingford
46. McQuarrie DA (2003) Statistical mechanics. VIVA, New Delhi
47. Laidler KJ (2004) Chemical kinetics, 3rd edn. Pearson Education, New Delhi
48. Brown RL (1981) J Res Natl Bur Stand 86:357–359
49. Xiao R, Noerpel M, Luk HL, Wei Z, Spinney R (2014) Int J Quantum Chem 114:74–83
50. Chuang YY, Truhlar DG (2000) J Chem Phys 112:1221–1228
51. Truhlar DG (1991) J Comput Chem 12:266–270
52. Kurylo MJ, Orkin VL (2003) Chem Rev 103:5049–5076